Chapter 6
Condition Monitoring for the Mounts of a Simple Supported Beam Using Transfer Path Analysis

Michael Kreutz and Daniel J. Rixen

Abstract Large machines like engines or turbines are subject to operational forces that may be hard to model or measure directly. Large machines are often connected to the environment via soft supports, which can degrade over time. Condition monitoring should detect and quantify changes in the dynamics of the joints to ensure the machine's performance. Transfer path analysis (TPA) can be used to characterize the unknown operational forces. Unlike in typical TPA, the characterization of the operational forces is not used to predict responses on the receiver system, but it is used together with measured operational responses to estimate frequency response functions (FRFs) of the system. These FRFs can be exploited in a frequency-based substructuring analysis to isolate and identify the joint dynamics. A numerical case study of a beam connected to the environments via discrete joints is used to validate this approach.

Keywords transfer path analysis · frequency-based substructuring · monitoring · joint identification

Introduction

Large machines, such as engines, turbines, and similar equipment, are often exposed to operational forces that are not fully understood. These machines are typically connected to their environment through multiple soft mounts (joints), which play a crucial role in vibration isolation and ensure the machine's proper function. However, the dynamics of these joints can change over time due to aging. In the context of condition monitoring, it is crucial to be able to detect and identify these changes in the joint dynamics during operation.

Transfer path analysis (TPA) is a method that considers the assembly of a source with an unknown excitation and a receiver structure. Typically, the goal of TPA is to characterize the excitation of the source and predict responses on the receiver. However, in the context of condition monitoring, the goal is different. From an equivalent force and a measured response, the dynamics (i.e., transfer functions, frequency response functions FRFs) of the system should be calculated. Using the calculated transfer functions on the machine, the joint dynamics can be extracted by using frequency-based substructuring.

This contribution presents a workflow to use TPA and frequency-based substructuring to identify in operation the mounts (called joints in this contribution) connecting a machine to a rigid environment. A numerical example of a beam with an operational excitation that is connected to the environments via spring-damper elements is used to validate the workflow. In a TPA step, the joints are considered as part of the receiver system and the beam is considered as source system. An equivalent force at the interface that represents the operational excitation is determined. Measurements of the response on the interface are used to obtain some transfer functions of the system at the interface. These transfer functions are then exploited in a frequency-based substructuring analysis to isolate the dynamics of the mounts.

Section 2 outlines the methodology. Section 3 presents a numerical case study of a beam in soft mounts to validate the method. Finally, a conclusion of the work and outlook for future studies is given.

Method

This section shortly introduces the TPA and the concept of equivalent forces, which is used to identify transfer functions of assembled systems. The identified transfer functions can be used to estimate the dynamics of a joint for a simplified system.

Michael Kreutz · Daniel J. Rixen
Chair of Applied Mechanics, TUM School of Engineering and Design, Technical University of Munich, Boltzmannstr. 15, 85748 Garching, Germany
e-mail: m.kreutz@tum.de; rixen@tum.de

© The Author(s), under exclusive license to River Publishers 2025

Walter D'Ambrogio, et al. (eds.), *Dynamic Substructuring & Transfer Path Analysis, Vol. 4*, Conference Proceedings of the Society for Experimental Mechanics Series, https://doi.org/10.13052/97887-438-0149-8_6

Transfer Path Analysis

An overview on transfer path analysis (TPA) can be found in [1, 2]. This section repeats the most important points of TPA.

Figure 1a present the setup of a TPA problem. The assembled system SR consists of an active source structure S with an unknown excitation $\boldsymbol{f}_1$ in degrees of freedom (dofs) 1 and a passive receiver structure R, where the responses $\boldsymbol{u}_3$ in dofs 3 should be predicted. The structures are connected in the interface with dofs 2. The excitation $\boldsymbol{f}_1$ is hard to be measured or modeled directly and is thus unknown. An example are the forces of a combustion engine that influence the noise-vibration harshness in a passenger car, cf. [3]. TPA aims at characterizing the excitation, identifying critical transfer paths and predicting the response on the receiver structure.

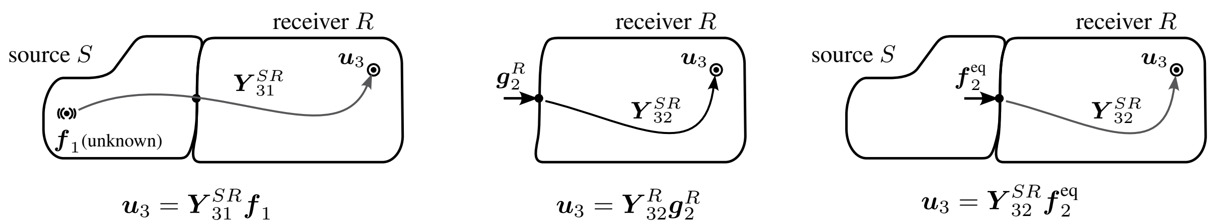

(a) Problem of TPA. (b) Classical TPA. (c) Component-based TPA.

Fig. 1 Overview of transfer path analysis, [1].

The *classical TPA* approach, see fig. 1b, tries to measure or estimate the internal forces in the interface 2 between the substructures. A disadvantage of the method is that those internal forces depend on the assembly and can thus not be reused if the receiver component is changed.

The *component-based TPA*, see fig. 1c, measures or estimates an equivalent force $\boldsymbol{f}_2^{\text{eq}}$ at the interface to represent the effect of the unknown excitation $\boldsymbol{f}_1$ on the responses $\boldsymbol{u}_3$ of the receiver:

$$\boldsymbol{u}_3 = \boldsymbol{Y}_{32}^{SR}\boldsymbol{f}_2^{\text{eq}} \tag{1}$$

The equivalent force can be measured on the source structure alone. The equivalent force is the opposite of the force at the interface, if the interface dofs are set to zero $\boldsymbol{u}_2 = 0$ (blocked). The equivalent force can also be found in-situ, by using response measurements and measured frequency response functions (FRFs) on the assembly, see [4]. Other methods to determine the equivalent force can be found in literature, e.g. in [1].

Applying the equivalent force $\boldsymbol{f}_2^{\text{eq}}$ on the interface of the assembled system has the same effect as the original excitation force $\boldsymbol{f}_1$. The equivalent force is a property of the source only and thus it is still valid even if the receiver structure is changed.

The workflow to apply component-based TPA is the following. The equivalent force $\boldsymbol{f}_2^{\text{eq}}$ is measured or estimated, for example as a blocked force of the source structure alone. It is also necessary to measure the FRFs $\boldsymbol{Y}_{32}^{SR}$ of the assembly SR from the interface dofs 2 to the response dofs 3. With this, we unknown responses $\boldsymbol{u}_3$ of the receiver can be estimated according to eq. (1).

Transmissibilty-based TPA is not presented here, but can be found in the literature (see e.g. [1, 2] for an overview).

Equivalent force for transfer function estimation

The idea of an equivalent force from component-based TPA is now used to estimate the FRFs of an assembled system.

Figure 2a shows the presented component-based TPA problem, where the goal is to estimate the response $\boldsymbol{u}_3$ using the equivalent force. Now, the problem is interpreted differently, see fig. 2b, in case it is possible to measure the response $\boldsymbol{u}_2$ or $\boldsymbol{u}_3$ in operation. Here, the goal is to estimate FRFs of the assembly. The previously measured or estimated equivalent force $\boldsymbol{f}_2^{\text{eq}}$ and the response $\boldsymbol{u}_2$ or $\boldsymbol{u}_3$ that is measured in operation are used in an FRF-estimator to obtain the FRFs $\boldsymbol{Y}_{22}^{SR}$ or $\boldsymbol{Y}_{32}^{SR}$ respectively. This idea has been used in [5].

To properly estimate the FRFs in a wide frequency range the equivalent forces must be broadband. This is not always the case, as $\boldsymbol{f}_2^{\text{eq}}$ is a consequence of the unknown operational forces $\boldsymbol{f}_1$, which may only excite some frequencies in practice.

If the interface is not described by a single dof but multiple dofs, a multiple-input multiple-output (MIMO) FRF-estimation has to be used. This presents the further requirements that the equivalent forces $\boldsymbol{f}_2^{\text{eq}}$ must be uncorrelated, cf. [6, p. 372]. As the equivalent forces depend on the dynamics of the source structure, some correlation cannot be avoided.

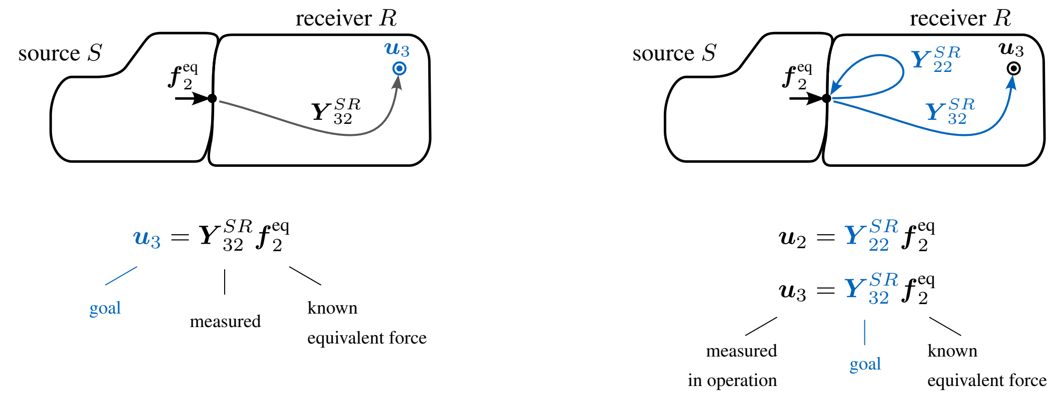

(a) Typical problem of component-based TPA, [1]. (b) For estimating transfer functions.

Fig. 2 Comparison of component-based TPA with FRF estimation using equivalent forces.

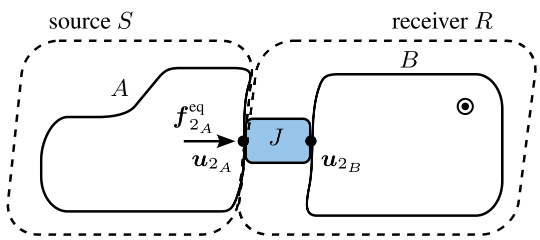

Fig. 3 Assembly AJB connected by a joint J and divided into a source S and a receiver R.

Towards condition monitoring of joints

With the presented method, the FRFs $\boldsymbol{Y}_{32}^{SR}$ and $\boldsymbol{Y}_{22}^{SR}$ can be measured in operation. As long as the source structure and the operational forcing $\boldsymbol{f}_1$ does not change, the equivalent force does not change, and the estimated FRFs are valid. This is even true, if the receiver system changes, as this does not influence the equivalent force $\boldsymbol{f}_2^{\text{eq}}$. With this, it is possible to observe changes in the estimated FRFs. The FRFs would change, if the dynamics of the receiver structure change. The current FRF that is measured during operation can be used for condition monitoring.

Figure 3 shows two substructures A and B that are connected via a joint J that can change and should be monitored. The structure A is considered the source structure S, while the part JB of the assembly is considered the receiver structure R. In a preliminary step, the equivalent force $\boldsymbol{f}_{2_A}^{\text{eq}}$ is measured or estimated. By measuring or estimating $\boldsymbol{u}_{2_A}$ and $\boldsymbol{u}_{2_B}$ during operation, a part of the FRF matrix of the assembly at the interface dofs can be estimated:

$$\begin{pmatrix} \boldsymbol{u}_{2_A} \\ \boldsymbol{u}_{2_B} \end{pmatrix} = \begin{pmatrix} \boldsymbol{Y}_{2_A,2_A}^{AJB} \\ \boldsymbol{Y}_{2_B,2_A}^{AJB} \end{pmatrix} \boldsymbol{f}_{2_A}^{\text{eq}} \tag{2}$$

Now this matrix is not the full interface FRF-matrix of the assembly, but only the columns corresponding to 2_A. So, it is for this general case not possible to directly apply the frequency-based substructuring techniques (that were used in [7]). For example, applying primal decoupling, would be not possible here, because an inversion of the submatrix $\boldsymbol{Y}_{2_A,2_A}^{AJB}$ corresponds to the condensation of the dynamics of AJB on point 2_A. It would not be possible to remove/decouple the dynamics of dynamic substructure B from this.

However, in the special case that the joint is quasi-static, the equations of dual coupling with a quasi-static joint (via a pseudo-inverse) can be rearranged to obtain the quasi-static joint. This idea was presented in [8], where FRF-measurements of internal points (away from the interface) were used. It is also possible to use only interface dofs, which can be seen in [9] and is given here shortly in the notation used in this paper. The coupling equation for a quasi-static joint to obtain the assembly FRF at dofs 2_A is given as:

$$\boldsymbol{Y}_{2_A,2_A}^{AJB} = \boldsymbol{Y}_{2_A,2_A}^{A} - \boldsymbol{Y}_{2_A,2_A}^{A}\left(\boldsymbol{Y}_{2_A,2_A}^{A} + \boldsymbol{Y}_{2_B,2_B}^{B} + \tilde{\boldsymbol{Y}}^{J}\right)^{-1}\boldsymbol{Y}_{2_A,2_A}^{A}, \quad \text{with} \quad \boldsymbol{u}_{2_B} - \boldsymbol{u}_{2_A} = \tilde{\boldsymbol{Y}}^{J}\boldsymbol{\lambda} \tag{3}$$

This equation can be rearranged to obtain the joint dynamics

$$\tilde{\boldsymbol{Y}}^J = \boldsymbol{Y}^A_{2_A,2_A}\left(\boldsymbol{Y}^A_{2_A,2_A} - \boldsymbol{Y}^{AJB}_{2_A,2_A}\right)^{-1}\boldsymbol{Y}^A_{2_A,2_A} - \boldsymbol{Y}^A_{2_A,2_A} - \boldsymbol{Y}^B_{2_B,2_B} \tag{4}$$

This requires additional measurements on the individual substructures A and B, but enables isolation of a quasi-static joint.

Estimation of joint dynamics connected to a rigid wall

Now, a special case is considered, where the source structure is connected to the environment via a joint, see fig. 4. This can be seen as replacing substructure B with a rigid wall. So, for this system, the full interface FRF matrix can be estimated,

$$\boldsymbol{u}_{2_A} = \boldsymbol{Y}^{AJB}_{2_A,2_A}\boldsymbol{f}^{\text{eq}}_{2_A}, \tag{5}$$

as for this case $\boldsymbol{u}_{2_B} = \boldsymbol{0}$ and thus $\boldsymbol{Y}^{AJB}_{2_A,2_B} = \boldsymbol{Y}^{AJB}_{2_B,2_A} = \boldsymbol{Y}^{AJB}_{2_B,2_B} = \boldsymbol{0}$. So, for this case a dynamic decoupling (frequency-based substucturing, see [2]) procedure can be applied that does not require the joint to be quasi-static.

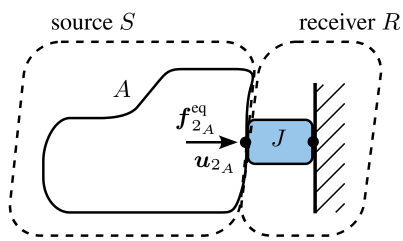

Fig. 4 Substructure A that is connected via a joint J to the rigid environment.

Here, a primal decoupling is applied to estimate the dynamic stiffness of the joint, see [2, 7],

$$\boldsymbol{Z}^J_{2_A,2_A} = \boldsymbol{Z}^{AJB}_{2_A,2_A} - \boldsymbol{Z}^A_{2_A,2_A}, \qquad \text{with} \quad \boldsymbol{Z}^{AJB}_{2_A,2_A} = \left(\boldsymbol{Y}^{AJB}_{2_A,2_A}\right)^{-1} \quad \text{and} \quad \boldsymbol{Z}^A_{2_A,2_A} = \left(\boldsymbol{Y}^A_{2_A,2_A}\right)^{-1}. \tag{6}$$

It is necessary to measure the FRF $\boldsymbol{Y}^A_{2_A,2_A}$ of substructure A, which has to be done on the disassembled structure, for example before the operation, when determining the equivalent forces. The resulting $\boldsymbol{Z}^J_{2_A,2_A}$ can be used to parameterize a simple physical model of the joint, e.g. as springs and dampers, cf. [7].

Numerical case study

The procedure presented in section 2.4 for a structure that is connected to the rigid environment via a joint is applied to a simulated example. First, the simulation setup is presented. Then the results for the estimation of the joint dynamics are given.

Simulation setup

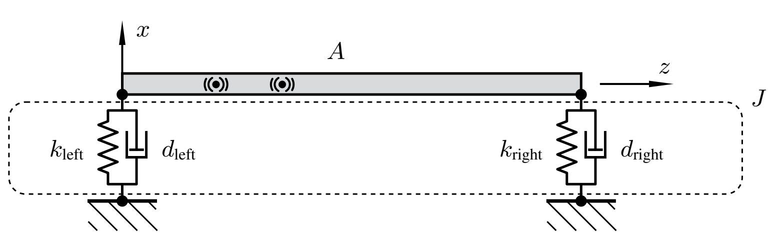

Fig. 5 Simulation setup.

The system consists of a 2D finite element TIMOSHENKO-beam which is connected to the environment via a spring-damper system on its left and right end, see fig. 5. The Young's modulus E, the density ρ, the Poisson-ratio ν, the length L, the diameter of the round cross-section d and the mesh size Δz are given as

$$E = 211 \cdot 10^9\,\mathrm{N\,m^{-2}}, \quad \rho = 7860\,\mathrm{kg\,m^{-3}}, \quad \nu = 0.3, \quad L = 0.5\,\mathrm{m}, \quad d = 0.01\,\mathrm{m}, \quad \Delta z = 0.01\,\mathrm{m}. \tag{7}$$

The parameters of the spring-damper elements are

$$k_{\text{left}} = 1 \cdot 10^6\,\mathrm{N/m}, \quad d_{\text{left}} = 100\,\mathrm{N\,s\,m^{-1}}, \qquad k_{\text{right}} = 2 \cdot 10^5\,\mathrm{N/m}, \quad d_{\text{right}} = 200\,\mathrm{N\,s\,m^{-1}}. \tag{8}$$

The operational forces $\boldsymbol{f}_1$ are applied in x-direction at positions $z = \begin{pmatrix} 0.05, & 0.2 \end{pmatrix}\,\mathrm{m}$ as constant spectrum with random phase in the frequency domain until 2000 Hz.

In the simulation model, the true equivalent force $\boldsymbol{f}^{\text{eq}}_{2_A}$ and the operational response $\boldsymbol{u}^{AJB}_{2_A}$ are computed in the frequency domain. They are then transformed in the time domain via an inverse fast Fourier transformation, where noise is added to the time signals. The transformation to the time domain is used, because in a real experimental application only time signals are measured directly. From the noisy time signals, the auto- and cross-power spectral densities are calculated using Welch's method and are given to a H_1-FRF-estimator. For these operations the free, open *Matlab*-toolbox *Abravibe* [10, 11] is used.

In detail, the steps for the simulated experiment are:

1. Obtain the equivalent force $\boldsymbol{f}_{2_A}$ from the source structure:

$$\boldsymbol{f}^{\text{eq}}_{2_A} = \left(\boldsymbol{Y}^{A}_{2_A,2_A}\right)^{-1} \boldsymbol{Y}^{A}_{2_A,1}\,\boldsymbol{f}_1 \tag{9}$$

   In an experimental application, the equivalent force would be measured, for example as blocked forces or in-situ.
2. Obtain the operational displacement $\boldsymbol{u}_{2_A}$ in the assembly:

$$\boldsymbol{u}_{2_A} = \boldsymbol{Y}^{AJB}_{2_A,1}\,\boldsymbol{f}_1 \tag{10}$$

   In an experimental application, this would be measured or estimated during the operation.
3. Transform $\boldsymbol{f}^{\text{eq}}_{2_A}$ and $\boldsymbol{u}_{2_A}$ in the time domain via an inverse FFT:

$$\tilde{\boldsymbol{f}}^{\text{eq}}_{2_A}(t) = \mathrm{IFFT}\left(\boldsymbol{f}^{\text{eq}}_{2_A}(\omega)\right), \qquad \tilde{\boldsymbol{u}}_{2_A}(t) = \mathrm{IFFT}\left(\boldsymbol{u}_{2_A}(\omega)\right) \tag{11}$$

   The time signals are periodically repeated and noise is added to simulate measurement noise.
4. Apply Welch's method to obtain auto- and cross power spectral densities and estimate $\boldsymbol{Y}^{AJB}_{2_A,2_A,\text{estim}}$ using an H_1-FRF-estimator, [6]:

$$\boldsymbol{Y} = \boldsymbol{G}_{\boldsymbol{yx}}\boldsymbol{G}^{-1}_{\boldsymbol{xx}}, \qquad \text{here, specifically:} \quad \boldsymbol{Y}^{AJB}_{2_A,2_A,\text{estim}} = \boldsymbol{G}_{\boldsymbol{u}_{2_A}\boldsymbol{f}^{\text{eq}}_{2_A}}\,\boldsymbol{G}^{-1}_{\boldsymbol{f}^{\text{eq}}_{2_A}\boldsymbol{f}^{\text{eq}}_{2_A}}, \tag{12}$$

   where $\boldsymbol{G}$ denotes an averaged auto or cross power spectral density. It can be seen that the input signal $\boldsymbol{x} = \boldsymbol{f}^{\text{eq}}_{2_A}$ should be uncorrelated, so that the inversion is well-conditioned.
   The same procedure would be applied in an experimental application.
5. Estimate the joint stiffness from $\boldsymbol{Y}^{AJB}_{2_A,2_A,\text{estim}}$

$$\boldsymbol{Z}^{J}_{2_A,2_A,\text{estim}} = \left(\boldsymbol{Y}^{AJB}_{2_A,2_A,\text{estim}}\right)^{-1} - \left(\boldsymbol{Y}^{A}_{2_A,2_A}\right)^{-1}. \tag{13}$$

   Select a clean frequency range in $\boldsymbol{Z}^{J}_{2_A,2_A,\text{estim}}$ and fit stiffness and damping in the real and imaginary part of $\boldsymbol{Z}^{J}_{2_A,2_A,\text{estim}}$ respectively for $\boldsymbol{Z}^{J}_{2_A,2_A,\text{identified}} = \mathrm{diag}\left(k_i + j\omega d_i\right)$.

Results

The correlation between two input signals x_n and x_m can be computed by

$$\gamma^2_{x_n,x_m} = \frac{|G_{x_n,x_m}|^2}{G_{x_n,x_n}G_{x_m,x_m}}, \tag{14}$$

where G_{x_n,x_n} and G_{x_m,x_m} are the auto-power spectral densities of x_n and x_m respectively and G_{x_n,x_m} is the cross-power spectral density between x_n and x_m. Figure 6 gives the correlation between the two entries of the blocked force $\boldsymbol{f}^{\text{eq}}_{2_A}$.

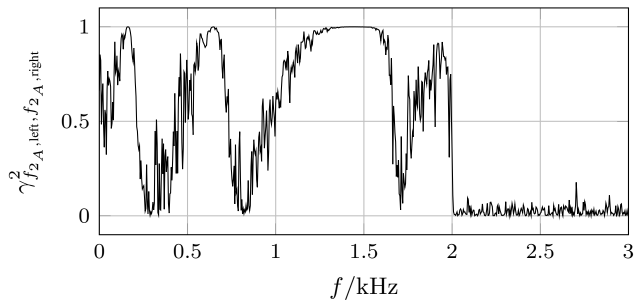

Fig. 6 Correlation $\gamma^2_{f_{2_A,\text{left}},f_{2_A,\text{right}}}$ between entries of equivalent force $\boldsymbol{f}^{\text{eq}}_{2_A}$.

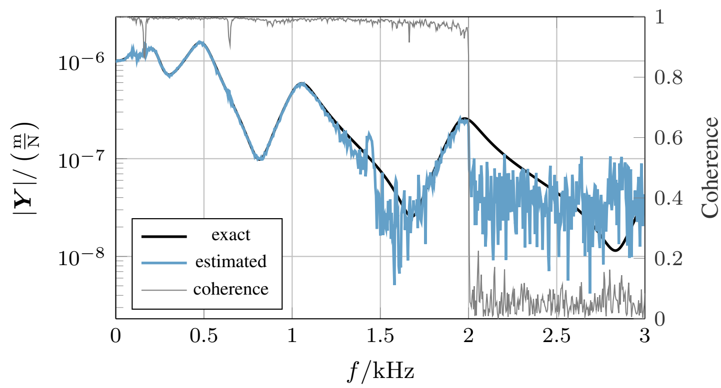

Fig. 7 Magnitude of the assembly FRF $|\boldsymbol{Y}^{AJB}_{2_A,2_A}|$ from estimation and exact values. Exemplary entry for excitation and response on the left side.

The correlation of the operational forces is not shown here, because it is zero for the entire frequency range meaning it is fully uncorrelated. This is the case, because we chose $\boldsymbol{f}_1$ to have a random phase in the frequency domain. Naturally, the correlation between the equivalent forces is not zero, because it depends on the dynamics of substructure A, see eq. (9). The FRF-estimation is ill-conditioned in regions with high correlation, because it involves an inversion of the auto power spectral density of the input, see eq. (12).

Figure 7 shows the estimated FRF $|\boldsymbol{Y}^{AJB}_{2_A,2_A,\text{estim}}|$ for the first diagonal entry and compares it to the exact values. Also, the multiple coherence for this FRF is given. It can be seen that the results agree well and that the coherence is high in the frequency range of excitation (until 2000 Hz). The effect of adding noise can be seen especially well in the region with low response amplitude. It should be noted that the effect of a large correlation between the equivalent forces seems to only have a negative effect on the coherence, where the correlation is almost one. These are the frequencies, where the coherence drops sharply in fig. 7.

Figure 8 shows the diagonal entries of the dynamic joint stiffness $\boldsymbol{Z}^{J}_{2_A,2_A}$ in real and imaginary parts. It gives the estimated and the exact values of $\boldsymbol{Z}^{J}_{2_A,2_A}$ and the fitted values in the marked frequency range. Additionally, the correlation between the input signal from fig. 6 is also plotted in the figure. The fitted stiffness and damping values and its deviation to the exact values is given in table 1. It can be seen that the identified stiffness and damping values agree very well for this example. It is very interesting that the values of $\boldsymbol{Z}^{J}_{2_A,2_A,\text{estim}}$ appear noisy or give bad results when the correlation between the input signals is bad. This is not obvious from looking at the coherence in fig. 7 which was good in the whole frequency range. So, to assess the quality of the identified stiffness, it is necessary to not only check the coherence of the estimated FRFs but also the correlation between the time signals. The correlation does not have to be exactly zero, as it can be seen that the estimated joint stiffness is also relatively clean in regions with some correlation between the input signals.

In appendix A, a case is considered, where only one force f_1 is applied on the beam at position $z = 0.05\,\text{m}$. This causes a very high correlation of the equivalent forces $\boldsymbol{f}^{\text{eq}}_{2_A}$. This causes a bad estimation of the assembly FRFs $\boldsymbol{Y}^{AJB}_{2_A,2_A,\text{estim}}$ and thus also of the estimated dynamic joint stiffness $\boldsymbol{Z}^{J}_{2_A,2_A,\text{estim}}$, which is why the joint identification fails for this case. This effect cannot be detected by the coherence of the FRF, but only through considering the correlation of the input signals.

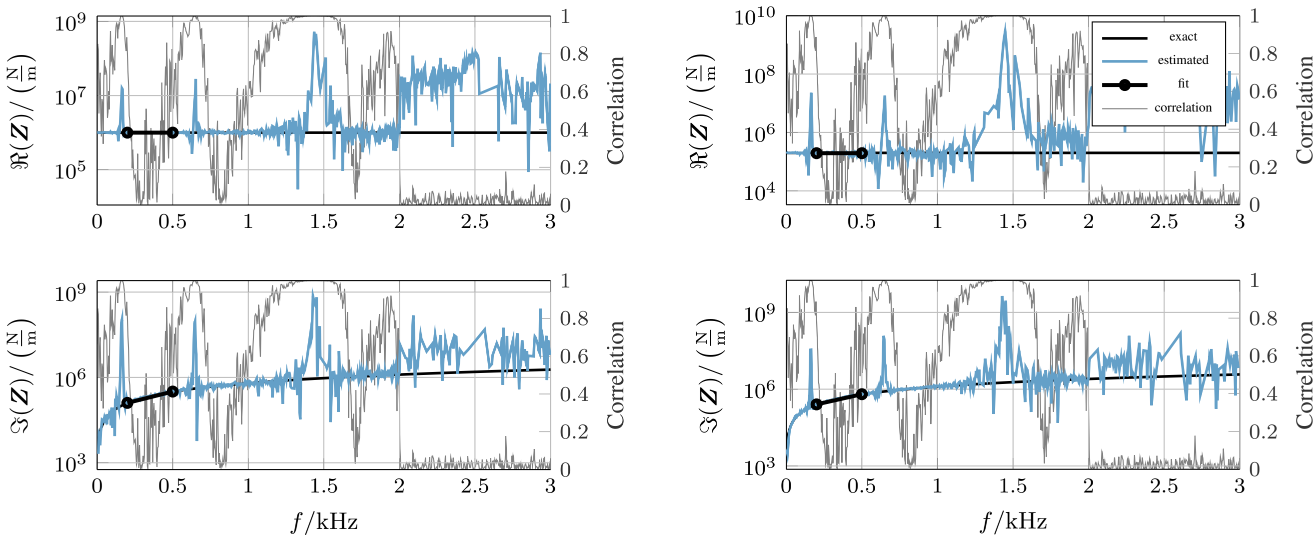

(a) Left joint: $\boldsymbol{Z}^{J}_{2_{A,\text{left}},2_{A,\text{left}}}$.

(b) Right joint: $\boldsymbol{Z}^{J}_{2_{A,\text{right}},2_{A,\text{right}}}$.

Fig. 8 Dynamic joint stiffness $\boldsymbol{Z}^{J}_{2_A,2_A}$.

Table 1 Identified stiffness and damping.

	exact value	estimated value	relative error
k_{left}	$1 \cdot 10^{6}\,\mathrm{N\,m^{-1}}$	$9.999 \cdot 10^{5}\,\mathrm{N\,m^{-1}}$	$-0.01\,\%$
d_{left}	$100\,\mathrm{N\,s\,m^{-1}}$	$101\,\mathrm{N\,s\,m^{-1}}$	$1.36\,\%$
k_{right}	$2 \cdot 10^{5}\,\mathrm{N\,m^{-1}}$	$1.951 \cdot 10^{5}\,\mathrm{N\,m^{-1}}$	$-2.45\,\%$
d_{right}	$200\,\mathrm{N\,s\,m^{-1}}$	$203\,\mathrm{N\,s\,m^{-1}}$	$1.37\,\%$

The presented difficulties due to a possible correlation naturally only occurs, when a MIMO-FRF-estimation is performed, i.e. if the joint has more than one dof. In the case, where only a single one-dof joint should be identified, the FRF estimation does not have these problems.

Conclusion and Outlook

This contribution presented a method to utilize the concept of equivalent forces, from component-based TPA, to estimate the FRFs of an assembly with a joint. In a simulation example of a simple supported beam, it was shown how this method can be used to estimate the dynamics of the mounts/joints from operational responses. This can be used in a condition monitoring to detect and quantify changes in the dynamics of the joints.

It was shown that the methods requires equivalent forces that are broadband, i.e. that excite a larger frequency range and it requires that the equivalent forces are sufficiently uncorrelated. The correlation is influenced by the correlation of the unknown operational forces and the dynamics of the active source structure. If the model of the joint is known, e.g. just a direct stiffness and damping, it may be enough if the correlation of the equivalent forces is low at some frequencies, but this was not investigated in detail here.

In a next step, the method should be applied on a real experimental example. It can be investigated how realistic operational forces lead to a correlation of the equivalent forces and thus the degradation of the joint identification. It can be discussed if the method can detect and quantify realistic changes in the joint parameters.

Another point that was not fully discussed in this contribution is how to estimate the joint dynamics for more complex assemblies, where the joint connects two flexible substructures.

Appendix: Results for high correlation of equivalent forces

In this section, the results for the presented simulation model in section 3 are given, when only one operational force $\boldsymbol{f}_1$ is applied. It can be seen that this leads to a high correlation of the equivalent forces, see fig. 10. In this case the FRF-estimation (fig. 9) and the decoupling of the joint stiffness (fig. 10) give bad results.

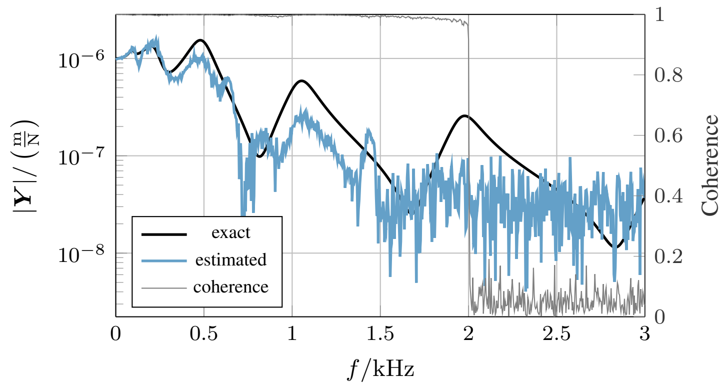

Fig. 9 Magnitude of the assembly FRF $|\boldsymbol{Y}^{AJB}_{2_A,2_A}|$ from estimation and exact values in the case of only one operational force f_1. Exemplary entry for excitation and response on the left side.

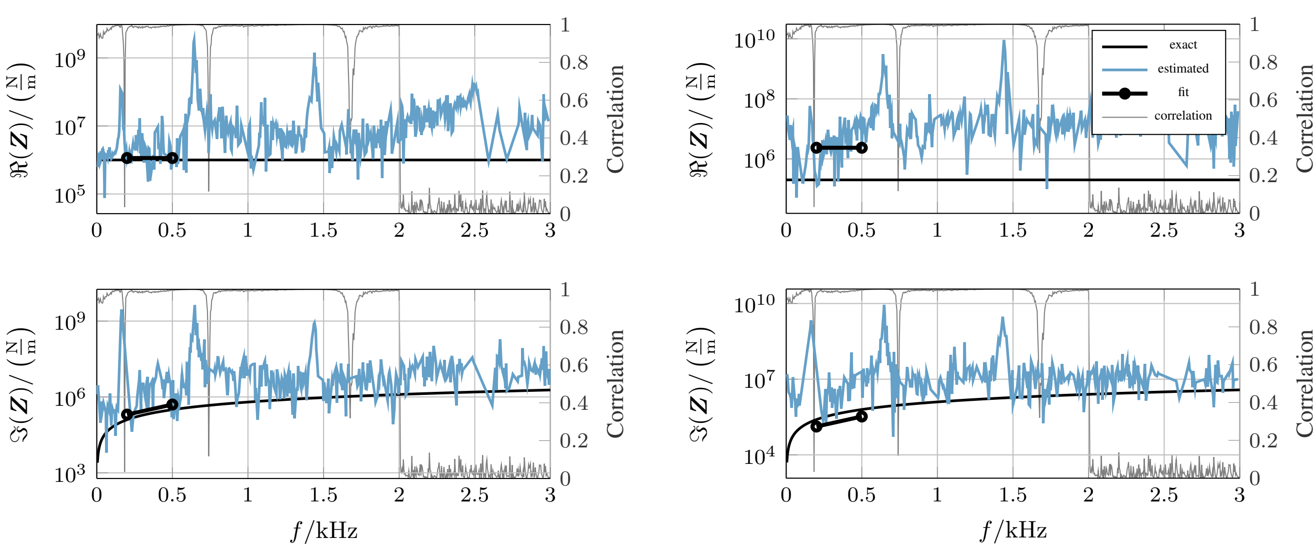

(a) Left joint: $\boldsymbol{Z}^J_{2_{A,\text{left}},2_{A,\text{left}}}$.

(b) Right joint: $\boldsymbol{Z}^J_{2_{A,\text{right}},2_{A,\text{right}}}$.

Fig. 10 Dynamic joint stiffness $\boldsymbol{Z}^J_{2_A,2_A}$ in the case of only one operational force f_1.

This example highlights the importance of checking the correlation of the input signals for the FRF-estimation. In the presented method, these are the equivalent forces $\boldsymbol{f}^{\text{eq}}_{2_A}$, see eq. (12).

References

[1] Seijs, M. V. van der, Klerk, D. de, and Rixen, D. J. "General framework for transfer path analysis: History, theory and classification of techniques". In: *Mechanical Systems and Signal Processing* 68-69 (2016), pp. 217–244. DOI: 10.1016/j.ymssp.2015.08.004.

[2] Allen, M. S., Rixen, D., Seijs, M. van der, Tiso, P., Abrahamsson, T., and Mayes, R. L. *Substructuring in Engineering Dynamics*. CISM International Centre for Mechanical Sciences. Cham: Springer International Publishing, 2020. DOI: 10.1007/978-3-030-25532-9.

[3] El Mahmoudi, A., Trainotti, F., Park, K., and Rixen, D. J. "In-Situ Source Characterization for NVH Analysis of the Engine-Transmission Unit". In: *Conference Proceedings of the Society for Experimental Mechanics Series*. Vol. 4. 2021, pp. 79–91. DOI: 10.1007/978-3-030-47630-4_7.

[4] Meggitt, J. and Moorhouse, A. "On the completeness of interface descriptions and the consistency of blocked forces obtained in situ". In: *Mechanical Systems and Signal Processing* 145 (Nov. 2020), p. 106850. DOI: 10.1016/j.ymssp.2020.106850.

[5] Ocepek, D., Vrtač, T., Čepon, G., and Boltežar, M. "Estimation of the frequency response functions for operational assemblies using independent source characterization". In: *Mechanical Systems and Signal Processing* 182.July 2022 (2023). DOI: 10.1016/j.ymssp.2022.109542.

[6] Brandt, A. *Noise and Vibration Analysis*. Second. Wiley, Oct. 2023. DOI: 10.1002/9781118962176.

[7] Kreutz, M., Trainotti, F., Gimpl, V., and Rixen, D. J. "On the robust experimental multi-degree-of-freedom identification of bolted joints using frequency-based substructuring". In: *Mechanical Systems and Signal Processing* 203 (Nov. 2023), p. 110626. DOI: 10.1016/j.ymssp.2023.110626.

[8] Özşahin, O., Ertürk, A., Özgüven, H. N., and Budak, E. "A closed-form approach for identification of dynamical contact parameters in spindle-holder-tool assemblies". In: *International Journal of Machine Tools and Manufacture* 49.1 (2009), pp. 25–35. DOI: 10.1016/j.ijmachtools.2008.08.007.

[9] Trainotti, F., Brøns, M., Klaassen, S., and Rixen, D. J. "Revisiting the Dual Admittance-Based Quasi-Static Formulation for the Identification of Linear Joint Dynamics with Dynamic Substructuring". In: *IMAC XLIII*. Orlando, FL, USA: Society for Experimental Mechanics, 2025.

[10] Brandt, A. "The ABRAVIBE toolbox for teaching vibration analysis and structural dynamics". In: *Conference Proceedings of the Society for Experimental Mechanics Series* 6 (2013), pp. 131–141. DOI: 10.1007/978-1-4614-6546-1_13.

[11] Brandt, A. *ABRAVIBE - A MATLAB toolbox for noise and vibration analysis*. www.abravibe.com. 2024.